Expert Systems With Applications 252 (2024) 124076

Contents lists available at ScienceDirect

Expert Systems With Applications

journal homepage: www.elsevier.com/locate/eswa

Simple analytical models for estimating the queue lengths from probe vehicles at traffic signals: A combinatorial approach for nonparametric models

Gurcan Comert[a,b,*], Tewodros Amdeberhan[c], Negash Begashaw[d], Negash G. Medhin[e], Mashrur Chowdhury[f]

[a] Computer Science and Engineering Department, Benedict College, 1600 Harden St., Columbia, SC 29204, USA
[b] Information Trust Institute, University of Illinois Urbana-Champaign, 1308 West Main St., Urbana, IL 61801, USA
[c] Department of Mathematics, Tulane University, 6823 St. Charles Avenue, New Orleans, LA 70118, USA
[d] Department of Mathematics, Benedict College, 1600 Harden St., Columbia, SC 29204, USA
[e] Department of Mathematics, North Carolina State University, Raleigh, NC 27695, USA
[f] Glenn Department of Civil Engineering, Clemson University, Lowry Hall, Clemson, SC 29634, USA

ARTICLE INFO

Keywords:
Cycle-to-cycle
Short-term
Connected vehicles
Combinatorics
Dynamic queue length estimation
Negative hypergeometric distribution

ABSTRACT

This study develops a combinatorial approach for nonparametric short-term queue length estimation in terms of cycle-by-cycle partially observed queues from probe vehicles (PV). The method does not assume random arrivals and does not assume any primary parameters or estimation of any parameters but uses simple algebraic expressions that only depend on signal timing. For an approach lane at a traffic intersection, the conditional queue lengths given probe vehicle location, count, time, and analysis interval (e.g., at the end of the red signal phase) are represented by a Negative Hypergeometric distribution. The simple analytical estimators obtained are compared with parametric methods from literature and highway capacity manual methods using field test data and simulation data involving probe vehicles. The analysis indicates that the nonparametric models presented in this paper match the accuracy of the parametric ones used in the field test and simulated data for estimating queue lengths.

1. Introduction

Probe vehicles (PV) or Lagrangian sensors can be considered as tracking-device-equipped vehicles that can report critical information (Hans, Chiabaut, & Leclercq, 2015) as they traverse transportation networks. Commercial taxis, volunteers, transit buses, maintenance vehicles, commercial trucks, etc., can report their location and timestamps through cellphones and GPS devices for improved traffic operations or better planning. The collected data can be used to estimate traffic parameters (e.g., flow, density, speed, queue lengths, and delays). The accuracy of these estimates depends on the quality of reported sensor data and the penetration of the number of data received from the vehicles. Regardless, observing mobile data from transportation networks gives critical coverage for dynamic traffic behavior. This study presents a method for estimating queue length given that (1) probe vehicles can be observed on a lane accurately and infer the order of vehicles in a queue, (2) we can deduce the beginning of queue start time to probe vehicle arrival times (e.g., relative to the beginning of red duration at a signal independent of signal control type), and (3) we can track the number of probe vehicles in the queue. Assuming these data are available, using the combinatorics approach, we develop cycle-to-cycle (dynamic) queue length estimators that can be used for any cyclic queues (e.g., signalized intersections) without requiring primary arrival rate or probe vehicle market penetration rate (or percentage) parameters.

In the previous related research, Herrera and Bayen developed improved traffic (i.e., flow and density) estimation models using cell phone-based probe vehicle data (Herrera & Bayen, 2010). The authors compared traffic flow theory and Kalman filter-based approaches. Ramezani and Geroliminis used high-resolution probe vehicle data to estimate travel time distribution after allocation and decomposition. The distribution could be used for reliability and report travel time from uncovered roadways (Ramezani & Geroliminis, 2012). Jenelius

* Corresponding author at: Computer Science and Engineering Department, Benedict College, 1600 Harden St., Columbia, SC 29204, USA.
E-mail addresses: gurcan.comert@benedict.edu (G. Comert), tamdeber@tulane.edu (T. Amdeberhan), negash.begashaw@benedict.edu (N. Begashaw), ngmedhin@ncsu.edu (N.G. Medhin), mac@clemson.edu (M. Chowdhury).

https://doi.org/10.1016/j.eswa.2024.124076
Received 6 August 2023; Received in revised form 16 November 2023; Accepted 19 April 2024
Available online 24 April 2024

and Koutsopoulos utilized low-frequency probe vehicles and spatial and temporal link features (more than 50 features) to estimate travel times (Jenelius & Koutsopoulos, 2013). The authors also show the effectiveness of low-frequency probe vehicle data estimating travel time distributions. The authors used theoretical travel time distributions used in the literature. Zheng et al. developed a stochastic model based on covariance dynamics for speed and density estimations and reported promising results after 20% probe vehicle proportions (Zheng, Jabari, Liu, & Lin, 2018). Duret and Yuan compared Eulerian (fixed loop detector) and Lagrangian (probe) and combined them for travel time estimation (Duret & Yuan, 2017). Authors reported that the above 10% probe proportion is needed for accurate estimations. Seo et al. estimated the fundamental diagram (flow-speed-density) behavior from probe vehicles, which can be used for planning or operations (Seo, Kawasaki, Kusakabe, & Asakura, 2019). Florin and Olariu also estimated density from probe vehicles using vehicles tracking the other passing vehicles (Florin & Olariu, 2020). Wang et al. estimated the queue profiles at signalized intersections using optimization and spatiotemporal shockwaves (Wang, Zhu, Ran, & Jiang, 2020). The study reported that 10%–20% probe proportion and 20–30 s sampling intervals would provide acceptable accuracy. In a similar study, the back of the freeway queue was estimated (Bae, Liu, Han, & Bozdogan, 2019).

Researchers have extensively studied the queue length estimation problem by proposing parametric (Zhao, Shen, & Liu, 2021; Zhao, Wong, Zheng & Liu, 2021; Zhao et al., 2019) and nonparametric methods. In this paper, we focused on the review of nonparametric ones. Jin and Ma presented a study on a nonparametric Bayesian method for traffic state estimation (Jin & Ma, 2019). In their study, they developed a generalized modeling framework for estimating traffic states at signalized intersections. The framework is nonparametric and data-driven, and no explicit traffic flow modeling is required. Wong et al. estimated the market penetration rate (probe proportion or percentage) (Wong, Shen, Zhao, & Liu, 2019). Based on probe vehicle data alone, they proposed a simple, analytical, nonparametric, and unbiased approach to estimate the penetration rate. The method fuses two estimation methods. One is from probabilistic estimation and the second is from samples of probe vehicles which is not affected by arrival patterns. It uses PVs and all vehicles ahead of the last PV in the queue.

Gao et al. presented queue length estimations (QLEs) based on shockwaves and backpropagation neural network (NN) sensing (Gao, Han, Dong, Xiong, & Du, 2019). The approach uses PV data and queue formation dynamics. It uses the shockwave velocity to predict the queue length of the non-probe vehicles. The NN is trained with historical PV data. The queue lengths at the intersection are obtained by combining the shockwave and NN-based estimates by variable weight. Tan et al. introduced License Plate Recognition (LPR) data in their study to fuse with the vehicle trajectory data and then developed a lane-based queue length estimation method (Tan, Liu, Wu, Cao, & Tang, 2020). The authors matched the LPR with probe vehicle data. They obtained the probability density function of the discharge headway and the stop-line crossing time of vehicles. They presented the lane-based queue lengths and overflow queues. Wang et al. proposed a QLE method on street networks using occupancy data (Wang, Bengler, Wets, & Niu, 2013). Their key idea is to use the speed decrease as the queue increase downstream of the loop detector. This would result in higher occupancy at constant volume-to-capacity ratios. Using VISSIM simulation, they generated data for various link lengths, lane numbers, and bus ratios. They fit a logistic model for the queue length and occupancy relationship. Then, queue lengths were estimated using multiple regression models. Van Phu et al. developed parametric estimators for the intersections with multiple lanes and showed effectiveness using microsimulations (Van Phu & Farhi, 2020). Then, the authors showed two two-stage models with estimators for primary parameters, arrival rate, and probe proportions (Van Phu & Farhi, 2022).

Contributions of this study

This paper aims to model cycle-to-cycle (i.e., dynamic) queue lengths at intersections generally without assuming random arrivals or any primary parameters (i.e., market penetration rate, arrival rate) or estimating these parameters.

1. Unlike fundamental non-parametric queue length estimations from arrival and service distributions (Goldenshluger, 2016; Goldenshluger & Koops, 2019; Schweer & Wichelhaus, 2015; Singh, Acharya, Cruz, & Quinino, 2021), our method uses mathematical techniques from combinatorics to derive discrete conditional probability mass functions of observed information about the queue and derive moments of the distributions without depending on probe vehicle proportion (i.e., the number of probe vehicle divided by all vehicles or also called market penetration rate), arrival, or service distributions. Thus, estimators derived can be used to calculate cycle-to-cycle queue length/delay values for signal timing or optimization.
2. As the title suggests, the paper builds on the authors' previous work. However, the approach presented in this study significantly extends the results from Comert (2013a), Comert and Cetin (2009) where Comert and Cetin (2009) presented a conditional probability mass function for probe location information and Comert (2013a) provided closed-form dynamic queue length estimators given probe vehicle location and time information. Both studies assumed Poisson arrivals. In this study, formulas do not assume any arrival distribution.
3. In this paper, derived estimators are the results of investigating the experiments, finding arrival distribution-free probability distributions, and obtaining mean and variance, which are direct estimators and errors. The results are simple and easy to use in any control framework. They can be used if queue start and end times are known or tracked (e.g., incident start and end, red signal start and end).
4. Proposed estimators do not consider random overflow queues, i.e., remaining queues from previous cycles, which can happen during random high arrival rates as volume-to-capacity ratio gets closer to 1.0.
5. Proposed estimators are valid for low to medium volume-to-capacity ratios (less than 0.80); thus, undersaturated conditions, meaning the queue is not building up after each cycle.

The paper is organized as follows: In Section 2, the approach is defined to set up derivations. In Section 3, we use combinatorial arguments and present a closed form of the sum of the probabilities in Eqs. (3) and (4). The result obtained in Section 3 enables us to define a probability mass function. We show that this probability distribution is Negative Hypergeometric. We use the results for the mean and variance of the distribution to derive formulas for the queue length estimators. In Section 4, we present numerical examples of the behavior of the derived estimators and show the performance of the estimators using field data. We summarize our findings and discuss possible future research directions in Section 5.

2. Problem definition

Probe vehicles (PVs) and partially observed systems through inexpensive sensors are facilitating real-time queue length estimations. Our goal in this paper is to model queue lengths (N) at intersections without assuming random arrivals or any primary parameters or estimating such parameters (i.e., arrival rate (λ) and probe vehicle market penetration rate (p)). In Fig. 1, a snapshot of an example queue (e.g., the waiting vehicles at the end of the red signal phase) is shown. Suppose that solid vehicles are observed. The total queue length N is written as a sum of two queues: the total number of vehicles up to the last probe

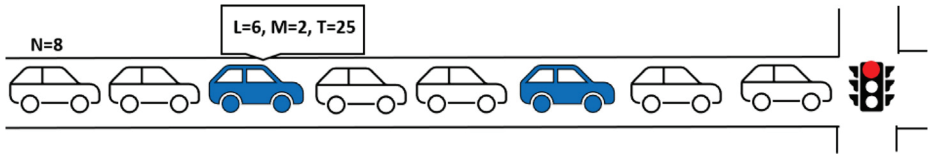

Fig. 1. Snapshot of an intersection at the end of a red phase.

N_1 and the number of vehicles after the last probe N_2. The estimator for the total queue length (N) given the location (L), the number of PVs (M) in the queue, the time of the last probe (T), and the signal timing (or time interval of interest (R)) can be expressed as follows.

$$E(N|L=l, M=m, T=t, R) = E(N_1|L=l, M=m, T=t, R) + E(N_2|L=l, M=m, T=t, R) \quad (1)$$

Now, the first part of the queue is trivial and equals the last probe vehicle location (order in the queue) $N_1 = l$ and the variance of the N_1 is $V(N_1|L=l, M=m, T=t, R) = 0$. After the last probe vehicle, N_2 contains uncertainty. If we simply assume Poisson arrivals $E(N_2|L=l, M=m, T=t, R) = (1-p)\lambda(R-t)$. And, if no initial queue (or overflow queue from the previous signal cycle) is assumed, the estimator becomes $E(N|L=l, M=m, T=t, R) = l + (1-p)\lambda(R-t)$. The essential information needed for the estimation is primary parameters such as flow rate (λ) and percent of probe vehicles (or market penetration rate p). However, both parameters are dynamic. Especially in real-time applications, like cycle-to-cycle or shorter-term queue lengths at signalized intersections, one would need to collect data for a few cycles to estimate these parameters. The parameters can then be updated and used in such applications. Assuming random arrivals, in Comert (2016), Comert and Begashaw (2022), it is shown that at least 10 cycles of PV data would be needed to start using queue length estimators.

If Poisson distribution is too restrictive, one can attempt to model the estimator as $E(N|L, M, T) = \sum_n np(N=n|L, M, T)$. This can be direct or using known or easier to identify simpler conditional distributions, e.g., Eq. (2). Please note that this approach would need to result in a simple algebraic form of estimators. Otherwise, calculations would be tedious.

$$p(N=n|l, m, t) = \frac{p(T=t|l, m, n)p(L=l|m, n)p(M=m|n)P(N=n)}{\sum_n p(T=t|l, m, n)p(L=l|m, n)p(M=m|n)P(N=n)} \quad (2)$$

For instance, the conditional probability of the location (order) of the last probe vehicle can be calculated by $p(L=l|M=m, N=n) = \binom{l-1}{m-1}/\binom{n}{m}$ given the number of probe vehicles and the total number of vehicles in the queue. In this probability mass function, L is the location of the last probe vehicle, M is the number of probe vehicles in the queue, and N is the total queue. In Fig. 1, L is 6, M is 2, and N is 8 vehicles. We can see that this approach does not assume any arrival pattern or parameter and only depends on probe vehicle data. Certainly, it is not taking advantage of queue joining time T of PVs with respect to signal timing. Note that T is assumed integer representing whole seconds or fine discrete sub-second time intervals. For signal timing, whole or half-second precision is commonly used in calculations (Urbanik et al., 2015). There is also the physical constraint of the vehicle following, which can be 0.5–2 s s even if vehicles arrive in a very closely following group.

This problem (i.e., derivation of conditional probability distribution given probe vehicle information) described as a single lane of approach can equivalently be expressed as Fig. 2 drawing balls labeled as arrival as a probe vehicle, arrival as a non-probe vehicle, or no arrival. Consider the approach lane queue formed in $2R$ (i.e., R is the red phase) time intervals where in a unit time interval, there can be, at most, one arrival. So, in this setup, there can be at most one arrival per 0.5 s. This can be thought of as the minimum possible time gap and can be updated in the formulations derived. For example, in Fig. 2, we have l arrivals within $2t$ discrete unit time intervals. Among these time intervals, $2t-1$ contain $m-1$ PVs, $2R-2t$ contain $n-l$ arrivals. Now, the problem is a negative inference, meaning n is changing as in Negative Binomial, so we are interested in $p(N=n|L=l, M=m, T=t, R)$, i.e., probability of having $N=n$ arrivals within R time interval given $L=l, T=t, M=m$. Calculating this probability, we obtain Eq. (3) or equivalently Eq. (4).

$$p(N=n|l, m, t, R) = \frac{\binom{2t}{l-m}\binom{2R-2t}{n-l}}{\binom{2R}{n-m}} \quad (3)$$

$$p(N=n|l, m, t, R) = \frac{\binom{n-m}{l-m}\binom{2R-(n-m)}{2t-(l-m)}}{\binom{2R}{2t}} \quad (4)$$

We can then calculate expected values to get the mean ($E(N=n|l, t, m, R)$ or the queue length estimator) and the variance ($V(N=n|l, t, m, R)$) of the estimator. However, we first need to

i. verify if this is a valid probability mass function,
ii. find the normalizing denominator for a valid probability mass function,
iii. simplify to forms that can be used as input–output models like, $E(N=n|l, t, m, R) = l + (1-p)\lambda(R-t)$ in Comert (2013b).
iv. show if this approach leads to one of the known negative probability mass functions (e.g., Negative Hypergeometric). This could facilitate (iii).

The above formulation approach would hold under certain conditions. Without claiming all, the following can be noted as some of the limitations of the study:

1. The paper models the cycle-to-cycle queue lengths at the end of red duration which is the maximum queue for deterministic queues. In real traffic signal queues when the signal turns green, there is a short loss time due to vehicle acceleration and reaction times. During this time, more vehicles can join the queue. Thus, we only estimate the total queue at the end of the red duration, not the maximum queue. They might slightly differ. Regardless, the formulations are valid if the start and end time of the analysis interval is known, e.g., the start and end times of red duration.
2. Undersaturated conditions are assumed, meaning, the queue is not building up after each cycle. In fact, the signal queue is cleared after each cycle, and sometimes overflow queues (remaining queues) are observed. Note that since the presence of PV in the queue is tracked, the estimators can show slightly overestimated results as overflow queue PVs are not from the same cycle arrivals. If the volume-to-capacity ratio gets higher (> 0.80), the expected queue length would have a significant overflow queue presence, thus, a long queue is expected. With more PVs present in the queue, estimators would show better results with $M=m$ and $L=l$ getting higher. The time information should be revised as it would be from a previous cycle. Overall, this can be corrected via scenario analysis (Comert, 2013b). However, it is not within the scope of this paper. For oversaturated conditions, the queue would grow steadily. In such cases, relative referencing of the probe vehicle information would be changed. The rate of queue growth could be estimated, and the unknown queue length after the last probe vehicle can be scaled accordingly.

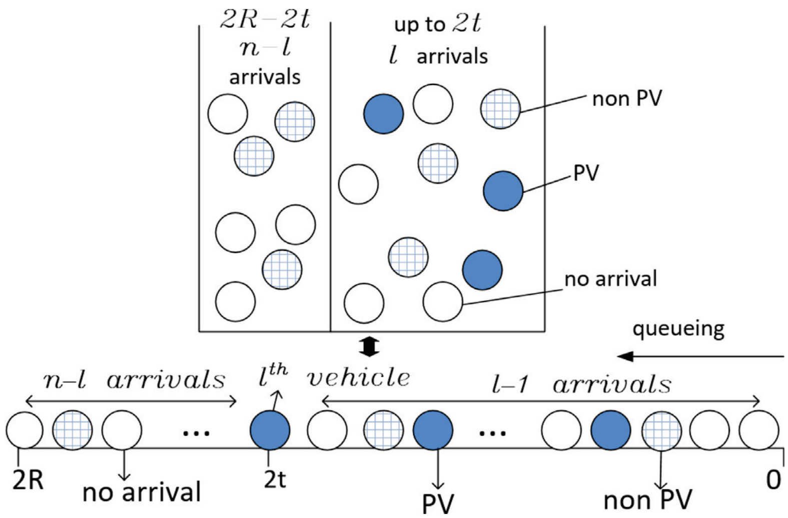

Fig. 2. Example queue with queue length, PV data, and arrival-no arrival spots.

3. How vehicles can be identified on a lane or limitations of GPS or tracking technology is not discussed. One can approach similarly to identify probe vehicles in a lane.

3. Probability mass function, expected value, and variance

We first provide combinatorial arguments and derive a closed form for the sum of the function in Eq. (4). Let ℓ, t, R, and m be as defined in the preceding section. Then

$$\sum_{n=\ell}^{2R-2t+\ell} \frac{\binom{n-m}{\ell-m}\binom{2R+m-n}{2t+m-\ell}}{\binom{2R}{2t}} = \frac{2R+1}{2t+1} \tag{5}$$

The complete derivation of Eq. (5) is provided in the Appendix under Theorem 1. We can see that the identity proved in the above theorem enables us to revise Eq. (4) and define a probability mass function. We can divide both sides of the identity by the expression on the right-hand side of the identity to get one on the right-hand side (i.e., the right-hand side of the identity is the normalizer of the probability distribution, which we explain below). Note that additional results from combinatorics and discussions are presented in Appendix.

In Negative Hypergeometric distribution (Johnson, Kemp, & Kotz, 2005), the probability of having k successes up to the rth failure given sample size of S and maximum possible queued vehicles K is given by

$$p(k|r,K,S) = \frac{\binom{k+r-1}{k}\binom{S-r-k}{K-k}}{\binom{S}{K}} \tag{6}$$

where S is the sample size (time capacity for arrivals and non-arrivals), K is the total number of successes (arrivals) in S, r is the number of failures (non-arrivals), and k is the number of successes (realizations of arrivals). The probabilities sum to 1. For the Negative Hypergeometric distribution, the expected value $E(k|r,K,S)$ and the variance $V(k|r,K,S)$ are given by Eqs. (7) and (8).

$$E(k|r,K,S) = \frac{rK}{S-K+1} \tag{7}$$

$$V(k|r,K,S) = \frac{rK(S+1)(S-K-r+1)}{(S-K+1)^2(S-K+2)} \tag{8}$$

In the probability mass function of the Negative Hypergeometric distribution (Eq. (6)), let $S = 2R+1$, $K = 2R-2t$, $r = l-m+1$, and $k = n-l$. Then the result proved in the theorem above gives the following probability mass function, which is a Negative Hypergeometric distribution since $\sum_{n=l}^{2R-2t+l}\binom{n-m}{l-m}\binom{2R+m-n}{2t+m-l} = \binom{2R+1}{2t+1}$. Notice that with these assignments arrivals and non-arrivals are fixed, and the probability of the total queue $N = n$ is calculated with known l, m, t, R.

$$p(N=n|l,m,t,R) = \frac{\binom{n-m}{l-m}\binom{2R+m-n}{2t+m-l}}{\binom{2R+1}{2t+1}} \tag{9}$$

From the formulas for the expected value and variance of the Negative Hypergeometric distribution, we get the following formulas for the expected value (Eq. (7)) and variance (Eq. (8)) of this probability distribution in Eq. (9). Note that $L = l, M = m, T = t, R$ are basic information from PVs, not primary parameters (arrival or penetration rate of probe vehicle in the traffic stream). We also do not require steady-state behavior if this Probe vehicle information is available. The expected queue length and its variance are short-term (R seconds or time interval) estimators.

The expected value $E(n|l,t,m,R)$ can be determined by

$$\begin{aligned} E(N=n|l,m,t,R) &= \sum_{n=l}^{2R-2t+l} \frac{n(2R+1)}{(2t+1)} \frac{\binom{n-m}{l-m}\binom{2R+m-n}{2t+m-l}}{\binom{2R+1}{2t+1}} \\ &= \sum_{n'=0}^{2R-2t} \frac{n'(2R+1)}{(2t+1)} \frac{\binom{n'+l'}{n'}\binom{2R-l'-n'}{2R-2t-n'}}{\binom{2R+1}{2t+1}} \end{aligned}$$

where $n' = n-l$, $l' = l-m$, and $\frac{(2R+1)}{(2t+1)}$ is the normalizer.

By Eqs. (7) and (8), simplified expected value or the queue length estimation 1 and the variance can be obtained as in Eqs. (10) and (11).

$$\begin{aligned} E(N_1 = n_1|l,m,t,R) &= l + \frac{(l-m+1)(2R-2t)}{2t+2} \\ &= l + \frac{(l-m+1)(R-t)}{t+1} \end{aligned} \tag{10}$$

$$V(N_1 = n_1|l,m,t,R) = \frac{(l-m+1)(2R+2)(2R-2t)}{(2t+2)(2t+3)}\left[1 - \frac{l-m+1}{2t+2}\right] \tag{11}$$

Alternatively, from Eq. (12), we can get the following equivalent estimator without PV time (T) information (Eq. (13)) and its variance in (Eq. (14)).

$$p(N=n|l,m,C) = \frac{\binom{C-n+m}{C-n}\binom{n-m}{n-l}}{\binom{C}{l}} \tag{12}$$

where C is capacity or maximum possible arrivals (e.g., $2R$ with 0.5 s headways), $J = C-2l$, $r = l-m+1$, $K = C-l$, and $k = n-l$. Note that, with time discretization, we can infer t from l. The expected value $E(n|l,m,R)$ is given by

$$E(N=n|l,m,C) = \sum_{n=l}^{C+l} \frac{n(l+1)}{(C+1)} \frac{\binom{C-n+m}{C-n}\binom{n-m}{n-l}}{\binom{C}{l}}$$

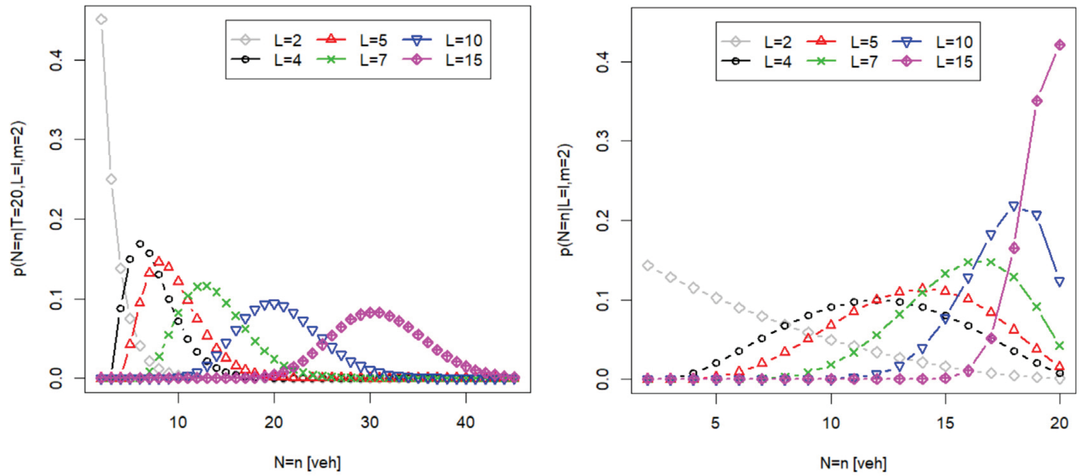

(a) $p(N = n|T = 20, L, M = 2, R = 45)$ in Eq. (9) (b) $p(N = n|L = l, M = 2, R = 45)$ in Eq. (12)

Fig. 3. Example behavior of conditional probabilities.

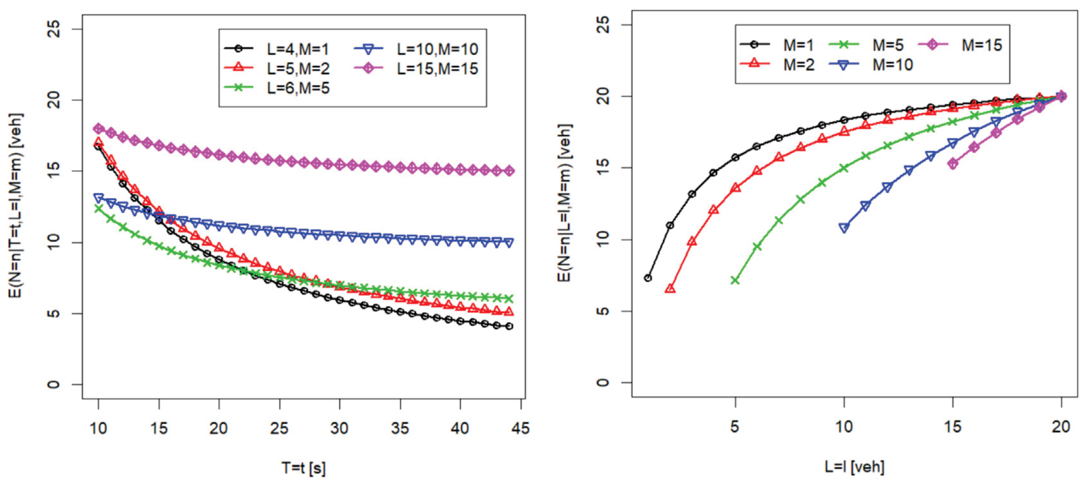

(a) $E(N|T, L, M = 2, R = 45)$ in Eq. (10) (b) $E(N|L, M, R = 45)$ in Eq. (13)

Fig. 4. Example behavior of conditional expectations.

$$= \sum_{n'=0}^{C} \frac{n'(l+1)}{(C+1)} \frac{\binom{n'+l'}{n'}\binom{C-l'+n'}{C-l'-n'}}{\binom{C}{n'}}$$

where $n' = n - l$, $l' = l - m$, and $\frac{(l+1)}{(C+1)}$ is the normalizer for valid probability mass function.

$$E(N_2 = n_2|l, m, C) = l + \frac{(l - m + 1)(C - l)}{l + 2} \tag{13}$$

$$V(N_2 = n_2|l, m, C) = \frac{(l - m + 1)(C + 2)(C - l)}{(l + 2)(l + 3)}[1 - \frac{l - m + 1}{l + 2}] \tag{14}$$

One of the advantages of the derived estimators in Eqs. (10) and (13) is that the denominators are nonzero since $L \geq 0$. This enables us to estimate queues even if there is no probe vehicle in the queue. The behavior of conditional probabilities, expected values, and variances are shown in Figs. 3–5. We can see in Fig. 3 that the likelihoods are right to the $N = l$ values. In Fig. 4, as the queue time joining of the last probe vehicle increases, the expected queue length gets closer to $L = l$ for both models. The variance of the conditional distributions is high. However, for these examples, $M = 2$. The variance will decrease when the number of PVs increases in the queue. Similarly, in Fig. 5, the variance of the estimated queue length reduces as l and t increase. Having time information also shows smoother behavior compared to having only location information.

Fig. 6 shows the percent coefficient of variation (CoV) with respect to T or L to understand errors relative to true average queue lengths. Suppose the maximum queue length is 20 vehicles per red duration (on average, the unconditional queue length is 16.52 vehicles), then, depending on the information M, L, the error is within 30% of the average queue length for the estimator with time information. Similarly, given information M, the error for the estimator without T is within 40% of the average queue length and decreases to zero as the location of the last probe increases. Note that the figures show the behavior of the conditional CoVs where M, L, T values are selected for illustrations. For other values, CoV values are going to change.

4. Evaluation with field queue length data

To show the effectiveness of the estimators developed, we used 2014 ITS World Congress Connected Vehicle Demonstration Data (CV Dataset, 2014). The authors' previous works used this field data for evaluating range sensor inclusion and filtering for queue length estimation (Comert & Begashaw, 2022; Comert & Cetin, 2021). The results of this study are new. For completeness, assumptions and setup are reported again. The dataset contains manually collected queue lengths at the intersection of Larned and Shelby streets in Detroit, Michigan,

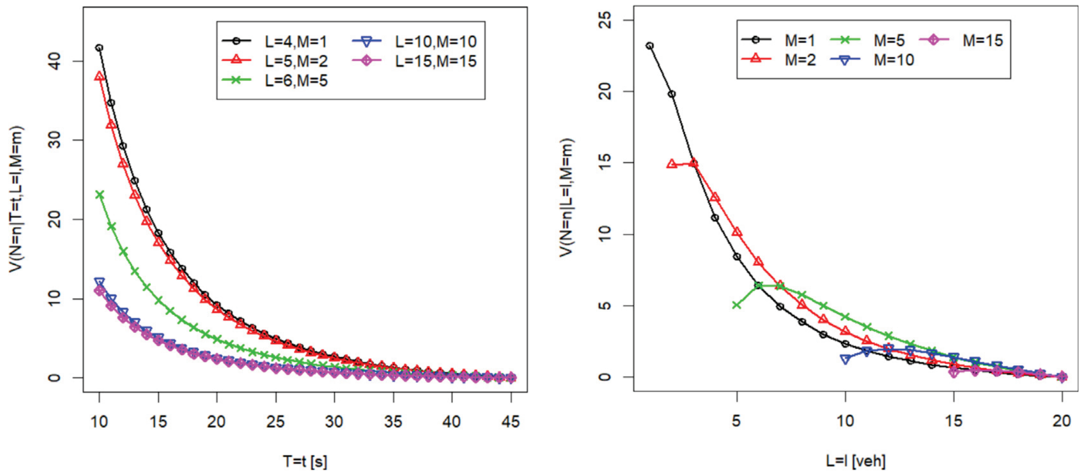

(a) $V(N|T,L,M=2,R=45)$ in Eq. (10)

(b) $V(N|L,M,R=45)$ in Eq. (14)

Fig. 5. Example behavior of conditional variances.

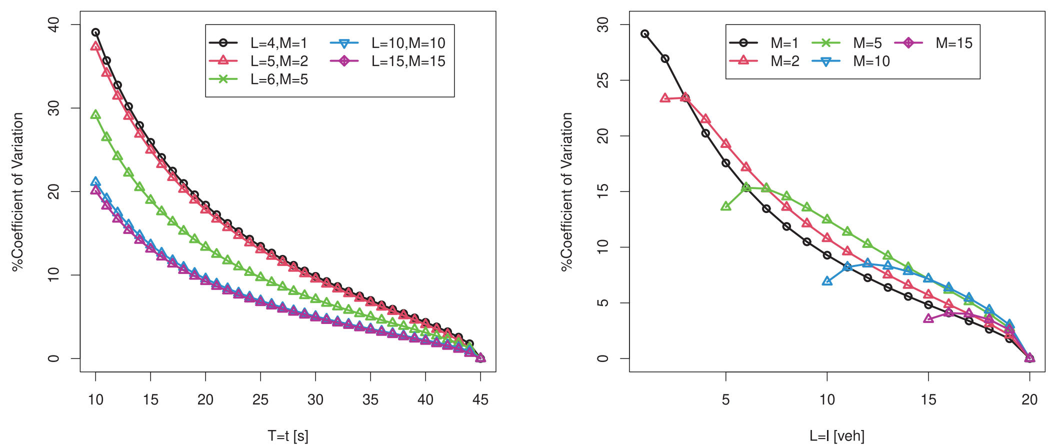

(a) $\frac{100*\sqrt{V(N|T,L,M=2,R=45)}}{E(N|T,L,M=2,R=45)}$

(b) $\frac{100*\sqrt{V(N|L,M,R=45)}}{E(N|L,M,R=45)}$

Fig. 6. Example behavior of conditional variances.

between September 8 and 10, 2014. The number of observations per day is 98, 254, and 135, respectively. During data collection, probe vehicles were identified with the blue Xs. Each row of data includes the hour, minute, and second of observation, the maximum queue lengths, and the number of probe vehicles in these queues (i.e., M in the formulations above) from the left, center, and right lanes of the Larned street approach.

The dataset provides $M = m$ and C cycle time values but not the information of L and T from PVs. Hence, we generated random variates of this information from Uniform distribution ($L = l$ location $l \sim U(m, n)$) and Gamma distribution ($T = t$ queue joining time $t \sim \mathcal{G}a(l, \frac{C}{2n})$) distributions for all lanes independently and repeated for 1000 random seeds. Note that, integer values are used for L, M, and T. The overall average of estimation errors is reported to compare models. In addition, the followings are assumed related to the traffic signal and the dataset:

1. Back-of-queue observations are obtained at the end of red phases (vary cycle-by-cycle). The time between two observations is assumed to be the cycle length (C), and red phases are assumed to be half ($R = C/2$).
2. There is no steady growth of queue and many zero queue values. Thus, the overflow queues are omitted. The data was collected during low to medium ρ (i.e., volume-to-capacity ratio= 0.50 assumed for HCM models). Please note this is real-life demo data from an urban arterial and is used to show the performance of the models against known parameters ones. Regardless, ρ's are also calculated using estimated arrival rates and used in relevant models.
3. The capacity of the approach was approximated by the observed overall maximum queue value of 10 vehicles within 70 s ($10 \times 3600/35 = 1029$ vehicles per hour or 0.286 vehicles per second (vps) saturation flow rate). These values are used essentially in the Highway Capacity Manual (HCM) from manual and back-of-queue calculations. Note that the values may not reflect the actual capacity and phase splits; however, we compare and report true queue lengths. This would provide insights into the accuracy of our approach.

Compared HCM delay (i.e., $Delay$ time difference between ideal versus actual conditions (or simply waiting time)) and back of the queue (i.e., $Qback$) models are given in Eqs. (15) and (16). These models are approximations for given time intervals (e.g., 15 min) and fully observed traffic.

$$d_1 = \frac{C}{2}[\frac{(1 - G/C)^2}{1 - [min(1, \hat{X})G/C]}]$$

Table 1
Estimators given for the queue lengths.

Estimator	$E(n\|l,m,t,R)$
Est.1	$I(m>0)[l+(l-m)(1-\frac{t}{R})]+I(m=0)[(1-\frac{\bar{m}}{\bar{l}})(\bar{l}+(\bar{l}-\bar{m})(1-\frac{\bar{t}}{R}))]$
Est.2	$I(m>0)[m+\frac{(l-m)R}{t}]+I(m=0)[\bar{m}+\frac{(\bar{l}-\bar{m})R}{\bar{t}}]$
NP.Est.1	$l+\frac{(l-m+1)(R-t)}{t+1}$
NP.Est.2	$l+\frac{(l-m+1)(C-l)}{l+2}$

$$d_2 = 900T[(\hat{X}-1)+\sqrt{(\hat{X}-1)^2+\frac{8kI\hat{X}}{cT}}] \tag{15}$$

where $d = d_1 \times PF + d_2 + d_3$ is control delay seconds per vehicle, d_2 is uniform delay, PF is progression factor due to arrival types, d_2 is random delay component, and d_3 is delay due to initial queue. In this study, only $d_1 + d_2$ are considered with $d_3 = 0$ since no overflow queue is assumed. $PF = 1.0$ is used for random arrivals. Volume-to-capacity is $\hat{X} = \hat{\rho} = \frac{\hat{\lambda}}{0.286}$. Green time G is in seconds s, C is cycle time in s. T is the analysis period in hours where in cycle-to-cycle estimations $T_i = C_i/3600$ is assumed where i denotes cycle number. k is incremental delay factor, and 0.5 is assumed for fixed time like movement. $I = 1$ upstream filtering is assumed for no interaction with nearby intersections, and capacity is $c = 1029\ vph$. Note that in our calculations, the uniform delay is the main component updated by changing G and C values. Queue lengths are approximated by Little's formula $d\lambda$ where d and λ are both calculated at each cycle using M number of probe vehicles in the queue. This method is based on HCM 2000 (Ni, 2020; Prassas & Roess, 2020).

Another estimation approach adopted from Kyte, Tribelhorn, et al. (2014) is used to calculate the cycle-to-cycle back of queues (see Eq. (16)).

$$Q_{back} = \hat{v}(R + g_s) \tag{16}$$

where Q_{back} is the back of the queue in vehicles, $v = \lambda$ is the arrival rate in vehicles per second (vps), R is the red duration in seconds s, and g_s is queue service time that is calculated $\hat{v}R/(x-\hat{v})$ with x is the saturation flow rate (i.e., assumed to be 0.286 vps). All the values R, g_s, and $\hat{v}$ except x are changing cycle-to-cycle.

Alternative estimators from Comert (2016) are denoted by Est.1 and Est.2 in Eqs. (17) and (18), respectively. These queue length estimators are in the form of $E(n|l,m,t,R) = l + (1-\hat{p})\hat{\lambda}(R-t)$ with two different primary parameter estimator combinations: $\{\hat{\lambda}_1 = \frac{l}{R}, \hat{p}_1 = \frac{m}{l}\}$ and $\{\hat{\lambda}_2 = \frac{(l-m)}{t} + \frac{m}{R}, \hat{p}_2 = \frac{mt}{mt+(l-m)R}\}$. All compared cycle-to-cycle queue length estimators are given in Table 1.

$$E(N_1|l,m,t,R) = I(m>0)[l+(l-m)(1-\frac{t}{R})]+ \\ I(m=0)[(1-\frac{\bar{m}}{\bar{l}})(\bar{l}+(\bar{l}-\bar{m})(1-\frac{\bar{t}}{R}))] \tag{17}$$

$$E(N_2|l,m,t,R) = I(m>0)[m+\frac{R(l-m)}{t}]+ \\ I(m=0)[(1-\frac{\bar{m}\bar{t}}{\bar{m}\bar{t}+(\bar{l}-\bar{m})R})(\bar{m}+\frac{R(\bar{l}-\bar{m})}{\bar{t}})] \\ = I(m>0)[m+\frac{(l-m)R}{t}]+I(m=0)[\bar{m}+\frac{(\bar{l}-\bar{m})R}{\bar{t}}] \tag{18}$$

where $I(.)$ is the indicator function. When there is no probe vehicle in the queue (i.e., $I(m=0)$), we use the average of previous probe vehicles' information as we need to estimate arrival rate (λ) and probe percentage (p). Notation $M_{1:i}$ represents values from cycle 1 to i and $\bar{m}_{1:i} = \sum_{j=1}^{i}\frac{m_j}{i}$, $\bar{l}_{1:i} = \sum_{j=1}^{i}\frac{l_j}{i}$, and $\bar{t}_{1:i} = \sum_{j=1}^{i}\frac{t_j}{i}$. Average error values are given in Table 2 for $T \sim \mathcal{G}a(l, \frac{C}{2n})$. Fig. 7(b) is given to demonstrate if assumed interarrivals are impacting the accuracy of the estimators.

In Table 2, a summary of average queue length (QL) estimation errors in the root mean square is provided (RMSE=$\sqrt{\sum_{i=1}^{n}\frac{(QL_i-\hat{QL}_i)^2}{n}}$).

Table 2
Estimation results with RMSE errors in [vehs/cycle] with $T \sim \mathcal{G}a(l, C/(2n))$.

	Lane	Avg. p	Est.1	Est.2	NP.Est.1	NP.Est.2	Delay	Q back
Sep08	L	13%	1.09	1.01	1.01	1.01	1.37	1.25
	C	21%	0.72	0.78	0.69	0.70	1.33	1.26
	R	7%	0.56	0.55	0.60	0.60	0.66	0.64
Sep09	L	10%	1.22	1.05	0.99	0.99	1.38	1.13
	C	26%	1.14	0.96	1.09	1.09	1.81	1.38
	R	2%	0.34	0.35	0.54	0.54	0.39	0.41
Sep10	L	7%	2.68	2.43	2.48	2.48	2.81	2.52
	C	18%	1.48	1.32	1.73	1.73	2.28	1.63
	R	1%	0.84	0.77	0.77	0.77	1.06	1.26

Average p values are calculated from $\sum_{i=1}^{n}\frac{m}{nQL_i}$ for each lane. Since true maximum queues are not known, p and λ are estimated. HCM's control delay-based model and back of queue are denoted by HCM_d and Q_{back}, respectively. The accuracy of the estimators is reported when probe vehicles are present in the queue ($p = \{10\%, 13\%, 18\%, 21\%, 26\%\}$).

Example performances with 21% penetration rates are given in Fig. 7(a). When there are probe vehicles in the queue, we can see that the proposed methods can follow the true maximum queue lengths closely. In Fig. 7(b), boxplots for overall errors are given. We can see that the model with new estimators provides slightly lower errors. However, errors are lower than delay-based HCM_d and Q_{back} methods. Our methods can estimate more accurately compared to Q_{back}.

4.1. Evaluation with simulated queue length data

In addition, the estimators are evaluated using Vissim microsimulations. The data from an isolated intersection is generated at five arrival rate levels $\lambda = \{7.34, 8.55, 9.81, 10.76, 12.02\}$ vehicles per 45 s red phase. For this intersection, capacity is 12.24 vehicles per 45 s and volume-to-capacity ratios are $\rho = \{0.60, 0.70, 0.80, 0.88, 0.98\}$. The cycle times are fixed at 90 s. There are no yellow or all-red phases. The probe proportion is changed between $p = \{0.001, 0.05, 0.10, .., 0.80, 0.999\}$ (i.e., 11 probe proportions). The simulation is run 1000 cycles for each probe proportion and arrival rate for three different random seeds (i.e., a total of 165,000 cycles of simulations).

Additional alternative estimators from Gao et al. (2019), Zhao et al. (2019) are denoted by $Est.3$ and $Est.4$ in Eqs. (19) and (20), respectively. These queue length estimators are in the form of $E(n|l,t,R) = l + \frac{l}{\bar{t}_{1:i}}(R-t)$ and $E(n|m,t) = \frac{t(m+1)}{m} - 1$. There are many other approaches; for simple comparison, the methods use the last probe vehicle's location, count, and time of arrival information are selected. With speed, density, and other probe information, and tracking all probe vehicles in the queue, additional estimators (Cheng, Qin, Jin, Ran, & Anderson, 2011; Luo, Deng, Chen, et al., 2023; Tiaprasert, Zhang, Wang, & Zeng, 2015) would also be compared.

$$E(N_3|l,t,R) = I(m>0)[l+\frac{l}{\bar{t}_{1:i}}(R-t)]+I(m=0)[\bar{l}_{1:i}+\frac{\bar{l}_{1:i}}{\bar{t}_{1:i}}(R-\bar{t}_{1:i})] \tag{19}$$

$$E(N_4|m,t) = I(m>0)[\frac{t(m+1)}{m}-1]+I(m=0)[\frac{\bar{t}_{1:i}(\bar{m}_{1:i}+1)}{\bar{m}_{1:i}}-1] \tag{20}$$

where $I(.)$ is the indicator function. When there is no probe vehicle in the queue (i.e., $I(m=0)$), we use the average of previous probe vehicles' information as at least one probe vehicle needed in the queue. Notation $m_{1:i}$ represents values from cycle 1 to i and $\bar{m}_{1:i} = \sum_{j=1}^{i}\frac{m_j}{i}$, $\bar{l}_{1:i} = \sum_{j=1}^{i}\frac{l_j}{i}$, and $\bar{t}_{1:i} = \sum_{j=1}^{i}\frac{t_j}{i}$.

The results, including all errors in RMSE and an example cycle-to-cycle queue length estimations, are given in Fig. 8. The results are consistent with the field test data. Note that field data is from a multi-lane intersection; the simulation data is from a single lane. The advantage of simulation is that p and λ are controlled. In this setup, compared estimators $Est.1$ and $Est.2$ have the advantage of finding

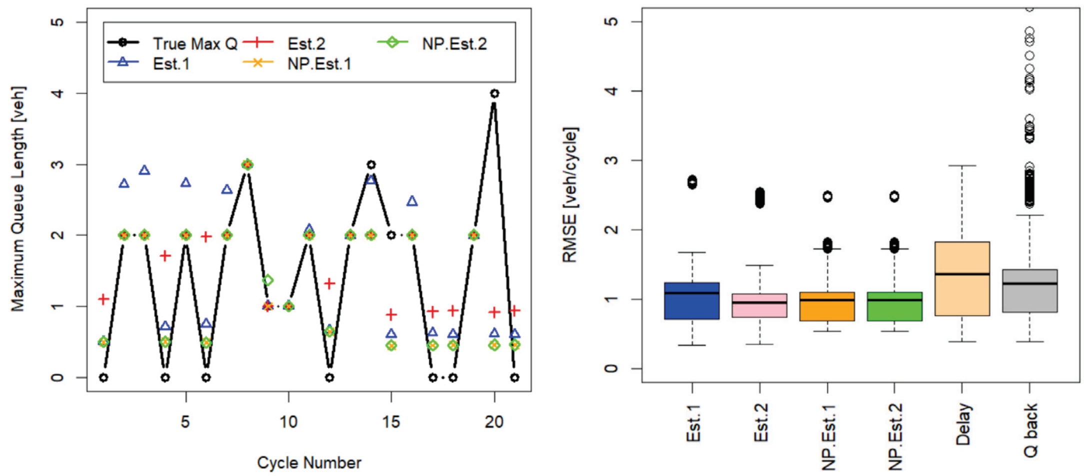

(a) Estimation on Sep 08 on center-lane

(b) Box plots for all estimation errors

Fig. 7. Performance of the proposed estimators $NP.Est.1$ and $NP.Est.2$.

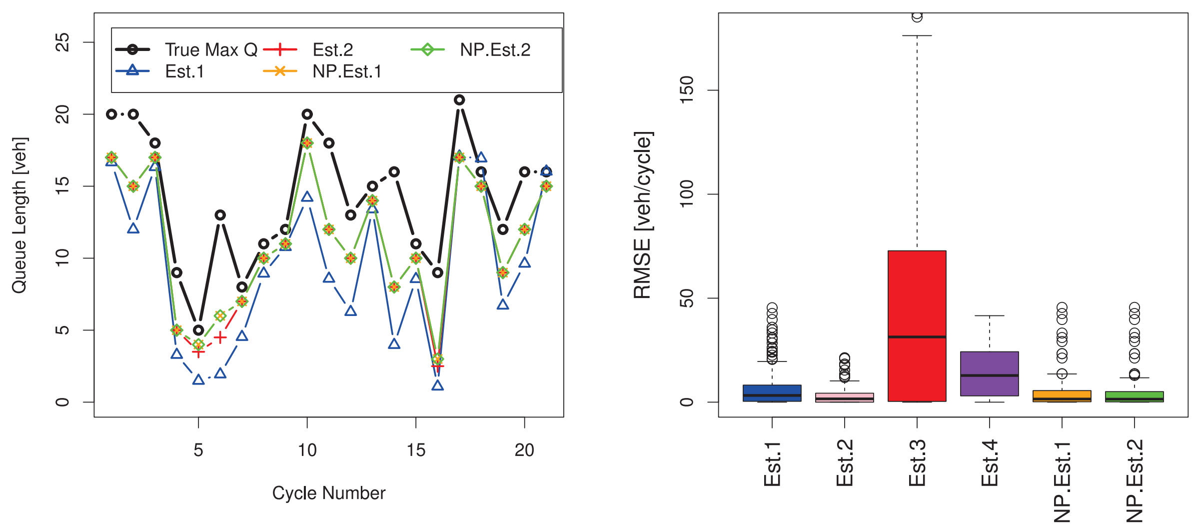

(a) Example estimation for $\lambda = 9.85$ and $p = 0.40$ levels

(b) Box plots for all estimation errors using simulated data

Fig. 8. Performance of the proposed estimators using simulated data.

true λ and p after a few cycles. When there is no probe vehicle at the intersection, they can use historical data. For proposed estimators and $Est.3$ and $Est.4$, they do not need λ or p. From the figure, it can be seen that the performance of $Est.2$ is approximately matched. Although they still produce larger estimation errors, the performance of $Est.3$ and $Est.4$ improves if average values are used instead of cycle-to-cycle probe vehicle information. We kept cycle-to-cycle estimation results in Fig. 8-b to compare them to proposed estimators.

Readers should note that the analysis and estimators in this paper do not consider overflow queues that can occur as the volume-to-capacity ratio gets higher $\rho > 0.80$. The outliers in Fig. 8-b may also directly result from the higher arrival rates and the overflow queues. Fig. 9 shows the increase in estimation errors from medium level $\rho = 0.70$ to $\rho = 0.98$. One can add simple corrections to the proposed estimators when preparing the data input, considering the following scenarios to elevate the impact.

a. If the last probe vehicle is in the overflow (remaining) queue, the signal cycle number can be tracked, and the first arrival to the queue can be noted. In this scenario, we can estimate overflow queue length and add another estimated queue for the new arrivals with no probe vehicle in them.
b. If the last probe vehicle is in the new arrivals, then the location information and number of probe vehicles would contain the overflow queue information. The estimators can be used as in Eqs. (10) and (13).
c. If no probe vehicle is in the queue, we can use values from previous cycles. These average probe information would contain the overflow queues' average impact depending on the number of times scenarios a and b were encountered.

5. Conclusions

In this study, we derived two new nonparametric cycle-to-cycle (i.e., dynamic) queue length estimation models for traffic signal-induced queues. Contributions can be summarized as follows:

i. Derived estimators only depend on signal phasing and timing information. The derivations involved fundamental analysis of the experiment.

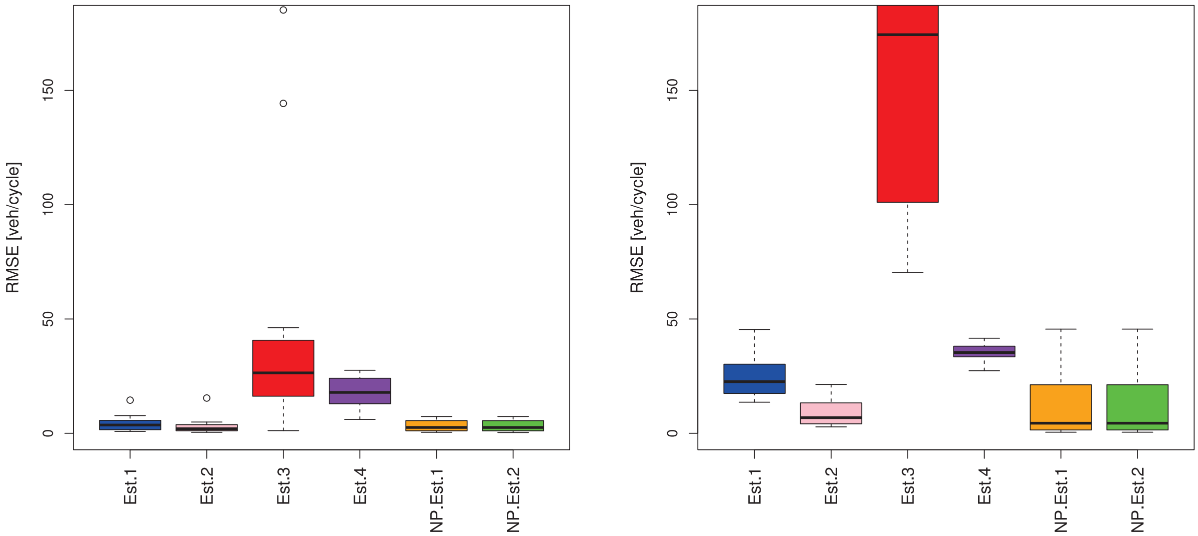

(a) Estimation errors for $\rho = 0.70$

(b) Estimation errors for $\rho = 0.98$

Fig. 9. Performance of the proposed estimators for medium and high ρ levels.

ii. One of the estimators ($NP.Est.2$, $E(N|l,m,R)$) does not require time information of the last probe vehicle in the queue and matches the accuracy of the one with time information ($NP.Est.1$, $E(N|l,m,t,R)$).
iii. Resulting estimators are simple algebraic expressions. We do not assume independent arrivals at the intersection. The only assumption is a discrete time interval, which is reasonable as signal timing involves whole seconds. However, sub-second or finer discrete time intervals can also be utilized.
iv. For independent approach lanes at traffic intersections, it is shown that conditional queue lengths given probe vehicle location, count, time, and analysis interval can be represented by a Negative Hypergeometric distribution.
v. Performance of the estimators derived was compared with parametric and simple highway capacity manual methods that use field test and simulated data involving probe vehicles. The results obtained from the comparisons show that the nonparametric models presented in this paper match the accuracy of parametric models. Compared parametric models assume known cycle-to-cycle (dynamic) arrival and market penetration rates.
vi. Methods developed do not assume random arrivals of vehicles at the intersection or any primary parameters or involve parameter estimations.

Developed methods in this study estimate the queue lengths at intersection approaches using probe vehicle data. These probe vehicles could be traditional probe vehicles or connected vehicles that generate basic safety messages. Apart from improving the limitations listed under the problem statement, future research could apply and expand the models presented in this paper using a more complex intersection and a series of adjacent intersections with higher traffic demand volumes.

CRediT authorship contribution statement

Gurcan Comert: Conceptualization, Derivations, Proofs, Methodology, Software, Visualization, Writing – original draft, Writing – review & editing. **Tewodros Amdeberhan:** Derivations, Combinatorics, Proofs. **Negash Begashaw:** Derivations, Proofs, Methodology, Investigation, Writing – original draft, Writing – review & editing. **Negash G. Medhin:** Derivations, Proofs, Writing – original draft, Writing – review & editing. **Mashrur Chowdhury:** Methodology, Investigation, Writing – original draft, Writing – review & editing.

Declaration of competing interest

The authors declare that they have no known competing financial interests or personal relationships that could have appeared to influence the work reported in this paper.

Data availability

Data will be made available on request.

Acknowledgments

This research was supported by the Center for Connected Multimodal Mobility, USA (C^2M^2) (USDOT Tier 1 University Transportation Center) and the National Center for Transportation Cybersecurity and Resiliency (TraCR), USA headquartered at Clemson University, Clemson, South Carolina, Department of Energy Minority Serving Institutions Partnership Program (MSIPP) managed by the Savannah River National Laboratory under BSRA contract TOA 0000525174 CN1, MSIPP-Claflin, FMCSA, FM-MHP-0678-22-01-00, NASA ULI (University of South Carolina-Lead), USA, National Science Foundation (NSF), USA Grants Nos. 1719501, 1954532, 2131080, 2200457, OIA-2242812, 2234920, and 2305470. Any opinions, findings, conclusions or recommendations expressed in this material are those of the authors and do not necessarily reflect the views of the Center for Connected Multimodal Mobility (C^2M^2) and the official policy or position of the USDOT/OST-R, or any State or other entity, and the U.S. Government assumes no liability for the contents or use thereof.

Appendix

Theorem 1. *Let ℓ, t, R, and m be as defined in the preceding section. Then*

$$\sum_{n=\ell}^{2R-2t+\ell} \frac{\binom{n-m}{\ell-m}\binom{2R+m-n}{2t+m-\ell}}{\binom{2R}{2t}} = \frac{2R+1}{2t+1} \tag{21}$$

or equivalently

$$\sum_{n=\ell}^{2R-2t+\ell} \binom{n-m}{\ell-m}\binom{2R+m-n}{2t+m-\ell} = \binom{2R+1}{2t+1} \tag{22}$$

Proof. Observe $\binom{n-m}{\ell-m}=\binom{n-m}{n-\ell}$ and $\binom{2R+m-n}{2t+m-\ell}=\binom{2R+m-n}{2R-2t-n+\ell}$ and replace $n'=n-\ell$ so that Eq. (4) becomes

$$\sum_{n'=0}^{2R-2t}\binom{n'+\ell-m}{n'}\binom{2R+m-n'-\ell}{2R-2t-n'}=\binom{2R+1}{2t+1} \tag{23}$$

Make another re-indexing $\ell'=\ell-m$ and hence Eq. (23) takes the form

$$\sum_{n'=0}^{2R-2t}\binom{n'+\ell'}{n'}\binom{2R-\ell'-n'}{2R-2t-n'}=\binom{2R+1}{2t+1} \tag{24}$$

The *"negativization"* (reminiscent of the Euler's *gamma reflection formula* $\Gamma(z)\Gamma(1-z)=\frac{\pi}{\sin(\pi z)}$) of binomial coefficients $\binom{-a+b}{b}=(-1)^b\binom{a-1}{b}$ allows to convert $\binom{\ell'+n'}{n'}=(-1)^{n'}\binom{-\ell'-1}{n'}$ and $\binom{2R-\ell'-n'}{2R-2t-n'}=\binom{2t-\ell'+2R-2t-n'}{2R-2t-n'}=(-1)^{2R-2t-n'}\binom{\ell'-2t-1}{2R-2t-n'}$. Therefore,

$$\begin{aligned}&\sum_{n'=0}^{2R-2t}\binom{n'+\ell'}{n'}\binom{2R-\ell'-n'}{2R-2t-n'}\\ &=\sum_{n'=0}^{2R-2t}\binom{-\ell'-1}{n'}\binom{\ell'-2t-1}{2R-2t-n'}\end{aligned} \tag{25}$$

The well-known *Vandermonde-Chu* identity states $\sum_{k=0}^{y}\binom{x}{k}\binom{z}{y-k}=\binom{x+z}{y}$. Applying this to Eq. (25) and engaging $\binom{-a+b}{b}=(-1)^b\binom{a-1}{b}$ (one more time) yields

$$\sum_{n'=0}^{2R-2t}\binom{-\ell'-1}{n'}\binom{\ell'-2t-1}{2R-2t-n'}=$$

$$\binom{-2t-2}{2R-2t}=(-1)^{2R-2t}\binom{2R+1}{2R-2t}=\binom{2R+1}{2t+1}$$

The proof is complete. □

Remark. The identity just proved shows that Eq. (3) or Eq. (4) is independent of the parameters m and ℓ. The results in Eq. 1 can be extended to the short sum runs from $n=\ell$ through $n=2R-2t$.

Theorem 2. *Let ℓ, m, n, R, and t be as defined in Theorem 1. Then there is a recurrence formula for*

$$\sum_{n=\ell}^{2R-2t}\binom{n-m}{\ell-m}\binom{2R+m-n}{2t+m-\ell} \tag{A5}$$

Proof. Denote the sum in (A5) by $f(\ell)$ and the summand by $F(\ell,n)$ (after suppressing the remaining variables). Introduce the function $G(\ell,n)=-\binom{n-m}{\ell+1-m}\binom{2R+m-n+1}{2t+m-\ell}$. Then, it is routine to verify that

$$F(\ell+1,n)-F(\ell,n)=G(\ell,n+1)-G(\ell,n) \tag{A6}$$

Sum both sides of (A6) for $n=\ell+1$ to $n=2R-2t$ (and telescoping on the right-hand side) to obtain

$$f(\ell+1)-f(\ell)+F(\ell,\ell)=G(\ell,2R-2t+1)-G(\ell,\ell+1).$$

Based on $F(\ell,\ell)=\binom{2R+m-\ell}{2t+m-\ell}$, $G(\ell,2R-2t+1)=-\binom{2R-2t-m+1}{\ell-m+1}\binom{2t+m}{\ell}$ and $G(\ell,\ell+1)=-\binom{2R+m-\ell}{2t+m-\ell}$, we infer the **recursive relation**

$$f(\ell+1)-f(\ell)=-\binom{2R-2t-m+1}{\ell-m+1}\binom{2t+m}{\ell}. \quad □$$

Corollary. From Theorem 2, we get the following identity

$$\sum_{\ell=0}^{2R-2t}\binom{2R-2t-m+1}{\ell-m+1}\binom{2t+m}{\ell}=\binom{2R+1}{2t+1} \tag{A7}$$

Proof. This follows from the recurrence relation proved in Theorem 2 and the identity proved in Theorem 1. □

Theorem 3. *The identity in (A7) can be re-indexed and formulated as follows:*

$$\sum_{m=\ell}^{R-t+\ell}\binom{m}{\ell}\binom{R-m}{t-\ell}=\binom{R+1}{t+1}.$$

Proof. We offer a combinatorial argument. Given natural numbers $\ell\le t\le R$, and m, we may consider the class of those $(t+1)$-subsets $\{x_0<x_1<\cdots<x_t\}$ of $\{0,1,\ldots,R\}$ such that $x_\ell=m$: these are exactly $\binom{m}{\ell}\binom{R-m}{t-\ell}$ (indeed the ℓ elements $x_0,\ldots,x_{\ell-1}$ can be chosen freely into $\{0,\ldots,m-1\}$, and so can the $t-\ell$ elements $x_{\ell+1},\ldots,x_t$ into $\{m+1,\ldots,R\}$. These classes, for $\ell\le m\le R-t+\ell$ form a partition of all $(t+1)$-subsets of $[R+1]$, whence the sum of their cardinality is independent of ℓ and the identity. □

Remark. The discrepancy in having a closed form and no closed form can be understood as follows: we know that $\sum_{k=0}^{n}\binom{n}{k}=2^n$, however, there is no "nice evaluation" for $\sum_{k=0}^{m}\binom{n}{k}$ unless $m=n$. The bottom line is the former is summed over the full compact support of $\binom{n}{k}$ (in the sense, $\binom{n}{k}=0$ if $k<0$ or $k>n$. A similar analogy can be drawn with having the closed form $\int_{\mathbb{R}}e^{-x^2}dx=\sqrt{\pi}$ but nothing similar is available if the limit is altered to be any smaller subset than the full range $\mathbb{R}$, except for $[0,\infty)$.

References

Bae, B., Liu, Y., Han, L. D., & Bozdogan, H. (2019). Spatio-temporal traffic queue detection for uninterrupted flows. *Transportation Research, Part B (Methodological)*, *129*, 20–34.

Cheng, Y., Qin, X., Jin, J., Ran, B., & Anderson, J. (2011). Cycle-by-cycle queue length estimation for signalized intersections using sampled trajectory data. *Transportation Research Record*, *2257*(1), 87–94.

Comert, G. (2013a). Effect of stop line detection in queue length estimation at traffic signals from probe vehicles data. *European Journal of Operational Research*, *226*(1), 67–76.

Comert, G. (2013b). Simple analytical models for estimating the queue lengths from probe vehicles at traffic signals. *Transportation Research, Part B (Methodological)*, *55*, 59–74.

Comert, G. (2016). Queue length estimation from probe vehicles at isolated intersections: Estimators for primary parameters. *European Journal of Operational Research*, *252*(2), 502–521.

Comert, G., & Begashaw, N. (2022). Cycle-to-cycle queue length estimation from connected vehicles with filtering on primary parameters. *International Journal of Transportation Science and Technology*, *11*(2), 283–297.

Comert, G., & Cetin, M. (2009). Queue length prediction from probe vehicle location and the impacts of sample size. *European Journal of Operational Research*, *197*(1), 196–202.

Comert, G., & Cetin, M. (2021). Queue length estimation from connected vehicles with range measurement sensors at traffic signals. *Applied Mathematical Modelling*, *99*, 418–434.

CV Dataset (2014). ITS world congress connected vehicle test bed demonstration vehicle situation data. URL http://data.transportation.gov. (Accessed 25 Jan 2021) from DOI: 10.21949/1504496.

Duret, A., & Yuan, Y. (2017). Traffic state estimation based on Eulerian and Lagrangian observations in a mesoscopic modeling framework. *Transportation Research Part B: Methodological*, *101*, 51–71.

Florin, R., & Olariu, S. (2020). Towards real-time density estimation using vehicle-to-vehicle communications. *Transportation Research Part B: Methodological*, *138*, 435–456.

Gao, K., Han, F., Dong, P., Xiong, N., & Du, R. (2019). Connected vehicle as a mobile sensor for real time queue length at signalized intersections. *Sensors*, *19*(9), 2059.

Goldenshluger, A. (2016). Nonparametric estimation of the service time distribution in the M/G/∞ queue. *Advances in Applied Probability*, *48*(4), 1117–1138.

Goldenshluger, A., & Koops, D. T. (2019). Nonparametric estimation of service time characteristics in infinite-server queues with nonstationary Poisson input. *Stochastic Systems*, *9*(3), 183–207.

Hans, E., Chiabaut, N., & Leclercq, L. (2015). Applying variational theory to travel time estimation on urban arterials. *Transportation Research, Part B (Methodological)*, *78*, 169–181.

Herrera, J. C., & Bayen, A. M. (2010). Incorporation of Lagrangian measurements in freeway traffic state estimation. *Transportation Research, Part B (Methodological)*, *44*(4), 460–481.

Jenelius, E., & Koutsopoulos, H. N. (2013). Travel time estimation for urban road networks using low frequency probe vehicle data. *Transportation Research, Part B (Methodological)*, *53*, 64–81.

Jin, J., & Ma, X. (2019). A non-parametric Bayesian framework for traffic-state estimation at signalized intersections. *Information Sciences*, *498*, 21–40.

Johnson, N. L., Kemp, A. W., & Kotz, S. (2005). *Univariate discrete distributions*: *vol. 444*, John Wiley & Sons.

Kyte, M., Tribelhorn, M., et al. (2014). *Operation, analysis, and design of signalized intersections: a module for the introductory course in transportation engineering*: *Technical report*, TranLIVE. University of Idaho.

Luo, H., Deng, M., Chen, J., et al. (2023). Queue length estimation based on probe vehicle data at signalized intersections. *Journal of Advanced Transportation*, *2023*, http://dx.doi.org/10.1155/2023/3241207.

Ni, D. (2020). *Signalized intersections*. Springer.

Prassas, E. S., & Roess, R. P. (2020). *The highway capacity manual: a conceptual and research history volume 2*. Springer.

Ramezani, M., & Geroliminis, N. (2012). On the estimation of arterial route travel time distribution with Markov chains. *Transportation Research, Part B (Methodological)*, *46*(10), 1576–1590.

Schweer, S., & Wichelhaus, C. (2015). Nonparametric estimation of the service time distribution in the discrete-time GI/G/∞ queue with partial information. *Stochastic Processes and their Applications*, *125*(1), 233–253.

Seo, T., Kawasaki, Y., Kusakabe, T., & Asakura, Y. (2019). Fundamental diagram estimation by using trajectories of probe vehicles. *Transportation Research, Part B (Methodological)*, *122*, 40–56.

Singh, S. K., Acharya, S. K., Cruz, F. R., & Quinino, R. C. (2021). Estimation of traffic intensity from queue length data in a deterministic single server queueing system. *Journal of Computational and Applied Mathematics*, *398*, Article 113693.

Tan, C., Liu, L., Wu, H., Cao, Y., & Tang, K. (2020). Fuzing license plate recognition data and vehicle trajectory data for lane-based queue length estimation at signalized intersections. *Journal of Intelligent Transportation Systems*, *24*(5), 449–466.

Tiaprasert, K., Zhang, Y., Wang, X. B., & Zeng, X. (2015). Queue length estimation using connected vehicle technology for adaptive signal control. *IEEE Transactions on Intelligent Transportation Systems*, *16*, 2129–2140.

Urbanik, T., Tanaka, A., Lozner, B., Lindstrom, E., Lee, K., Quayle, S., et al. (2015). *Signal timing manual*: *vol. 1*, DC: Transportation Research Board Washington.

Van Phu, C. N., & Farhi, N. (2020). Estimation of urban traffic state with probe vehicles. *IEEE Transactions on Intelligent Transportation Systems*, *22*(5), 2797–2808.

Van Phu, C. N., & Farhi, N. (2022). Estimation of road traffic state at a multilanes controlled junction. *IEEE Transactions on Intelligent Transportation Systems*, *23*(12), 23657–23667.

Wang, W., Bengler, K., Wets, G., & Niu, H. (2013). Modeling and simulation in transportation engineering. *Mathematical Problems in Engineering*, *2013*, 1–2.

Wang, Z., Zhu, L., Ran, B., & Jiang, H. (2020). Queue profile estimation at a signalized intersection by exploiting the spatiotemporal propagation of shockwaves. *Transportation Research Part B: Methodological*, *141*, 59–71.

Wong, W., Shen, S., Zhao, Y., & Liu, H. X. (2019). On the estimation of connected vehicle penetration rate based on single-source connected vehicle data. *Transportation Research, Part B (Methodological)*, *126*, 169–191.

Zhao, Y., Shen, S., & Liu, H. X. (2021). A hidden Markov model for the estimation of correlated queues in probe vehicle environments. *Transportation Research Part C (Emerging Technologies)*, *128*, Article 103128.

Zhao, Y., Wong, W., Zheng, J., & Liu, H. X. (2021). Maximum likelihood estimation of probe vehicle penetration rates and queue length distributions from probe vehicle data. *IEEE Transactions on Intelligent Transportation Systems*, *23*(7), 7628–7636.

Zhao, Y., Zheng, J., Wong, W., Wang, X., Meng, Y., & Liu, H. X. (2019). Various methods for queue length and traffic volume estimation using probe vehicle trajectories. *Transportation Research Part C (Emerging Technologies)*, *107*, 70–91.

Zheng, F., Jabari, S. E., Liu, H. X., & Lin, D. (2018). Traffic state estimation using stochastic Lagrangian dynamics. *Transportation Research, Part B (Methodological)*, *115*, 143–165.